

South Dakota State University
Open PRAIRIE: Open Public Research Access Institutional
Repository and Information Exchange

GSCE Faculty Publications

Geospatial Sciences Center of Excellence (GSCE)

7-2016

Best practices for the Reprojection and Resampling of Sentinel-2 Multi Spectral Instrument Level 1C Data

David P. Roy

South Dakota State University, david.roy@sdstate.edu

Jian Li

South Dakota State University, Jian.Li@sdstate.edu

Hankui Zhang

South Dakota State University, hankui.zhang@sdstate.edu

Lin Yan Dr.

South Dakota State University, lin.yan@sdstate.edu





Follow this and additional works at: https://openprairie.sdstate.edu/gsce_pubs

Recommended Citation

Roy, David P.; Li, Jian; Zhang, Hankui; and Yan, Lin Dr., "Best practices for the Reprojection and Resampling of Sentinel-2 Multi Spectral Instrument Level 1C Data" (2016). *GSCE Faculty Publications*. 40.
https://openprairie.sdstate.edu/gsce_pubs/40

This Article is brought to you for free and open access by the Geospatial Sciences Center of Excellence (GSCE) at Open PRAIRIE: Open Public Research Access Institutional Repository and Information Exchange. It has been accepted for inclusion in GSCE Faculty Publications by an authorized administrator of Open PRAIRIE: Open Public Research Access Institutional Repository and Information Exchange. For more information, please contact michael.biondo@sdstate.edu.

Best practices for the reprojection and resampling of Sentinel-2 Multi Spectral Instrument Level 1C data

David P. Roy , Jian Li , Hankui K. Zhang  and Lin Yan 

Geospatial Sciences Center of Excellence, South Dakota State University, Brookings, SD, USA

ABSTRACT

The standard geolocated Sentinel-2 Multi Spectral Instrument (MSI) L1C data products are defined in spatially overlapping tiles in different Universal Transverse Mercator (UTM) map projection zones. Best practices for reprojection and resampling to properly utilize and benefit from the L1C data format are presented. Three sets of 10 m Sentinel-2 L1C data acquired in the same orbit at different latitudes are examined to illustrate and quantify (a) the spatial properties of the L1C data and provide insights into the occurrence of overlapping tiles and overlapping tiles defined in different UTM zones from the same MSI swath, (b) the geometric implications of resampling and reprojection approaches that consider only the data from one L1C tile and not the data from other tiles in the overlap region that are defined in different UTM zones and (c) a recommended approach that considers all the overlapping L1C tile data and is shown statistically and qualitatively to improve the geometric fidelity of the projected resampled L1C data.

ARTICLE HISTORY

Received 19 May 2016

Accepted 7 July 2016

1. Introduction

The Sentinel-2 Multi Spectral Instrument (MSI) has 13 reflective spectral bands defined at 10 m, 20 m and 60 m in an approximately 290 km swath (20.6° field of view from an altitude of 786 km) with global coverage every 10 days (Drusch et al. 2012). The data are processed into top-of-atmosphere (TOA) radiance swath (L1B) products, that are not currently available and are designed for expert users who can undertake complex orthorectification themselves, and as available geolocated TOA reflectance (L1C) products (ESA 2015a, 2015b). The geolocated L1C products are defined by splitting each MSI swath into fixed 109 × 109 km tiles in the Universal Transverse Mercator (UTM) map projection. The L1C tile structure is quite complicated for users to handle without reliance on dedicated software tool kits. In particular, as we illustrate in this article, adjacent L1C tiles from the same MSI swath overlap spatially and may be defined in different UTM zones, i.e., in separate map projections each covering 6° of longitude centred over a meridian of longitude (Snyder 1993).

The correct handling of spatially overlapping L1C tiles defined in different UTM zones is required to properly utilize and benefit from the Sentinel-2 L1C format. We demonstrate that reprojection approaches that consider only the data from one L1C tile, and

CONTACT David P. Roy  david.roy@sdsu.edu  Geospatial Sciences Center of Excellence, South Dakota State University, Brookings, SD 57007, USA

© 2016 The Author(s). Published by Informa UK Limited, trading as Taylor & Francis Group. This is an Open Access article distributed under the terms of the Creative Commons Attribution-NonCommercial-NoDerivatives License (<http://creativecommons.org/licenses/by-nc-nd/4.0/>), which permits non-commercial re-use, distribution, and reproduction in any medium, provided the original work is properly cited, and is not altered, transformed, or built upon in any way.

not also from overlapping tiles defined in different UTM zones from the same MSI swath, will result in a pronounced degradation of the geometric fidelity. A computationally efficient approach that considers all the L1C tile data is described. This is important because we demonstrate the occurrence of overlapping tiles defined in different UTM zones is common and because L1C data reprojection is needed to make regional to global scale map products or to compare the data to other satellite data (Roy et al. 2010; Yan et al. 2016).

2. Study area and data

The Sentinel-2 L1C data are provided in Standard Archive Format for Europe (SAFE) files (ESA 2015a, 2015b). Each SAFE file corresponds to approximately 45 s of MSI sensing in the track direction, covering approximately 290 km (across-track) by 325 km (along-track). There are typically more than 10 L1C tiles in each SAFE file. Three SAFE files were acquired from the same Sentinel-2 orbit to (a) ensure that only images sensed on the same day were acquired, and so temporal compositing of images from different days (Roy et al. 2010, 2014; Griffiths et al. 2013) is not required; (b) capture a range of latitudes, as the overlap between adjacent UTM zone changes polewards and (c) reduce different geometric errors that can be present in different polar orbiting satellite orbits (Wolfe et al. 2002). Figure 1 shows a screenshot of the Sentinels Scientific Data Hub and the locations of the three selected SAFE files. The SAFE files were sensed on 8 December 2015 over the Russian Federation (south east of Moscow), Sudan (north of Magrur) and South Africa (Cape Town).

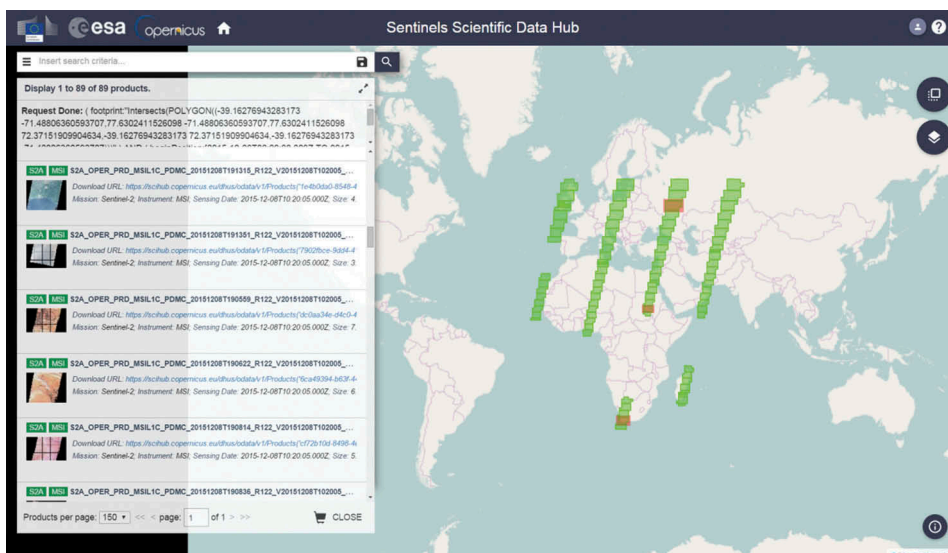


Figure 1. Sentinels Scientific Data Hub screen shot (<https://scihub.copernicus.eu/>) showing the locations of the three SAFE files used in this study. Green shows the Sentinel-2 locations sensed 8 December 2015 and orange shows the three selected images used in the Russian Federation (centre 52°43'44.4"N 42°52'22.8"E), Sudan (centre 14°48'28.8"N 30°58'30.0"E) and South Africa (centre 33°55'48.0"S 19°47'52.8"E). The data were ordered on 2 February 2016.

3. Methodology

3.1. Map projection and tile coordinate system

A map projection and coordinate system was selected. The specific map projection is unimportant for the purposes of this study as resampling effects will occur at the scale of several 10 m Sentinel L1C pixels, and at this local scale, geometric distortions imposed by different map projections are negligible (Snyder 1993). The equal area sinusoidal projection used to define the global coarse spatial resolution Moderate Resolution Imaging Spectroradiometer (MODIS) land products (Wolfe, Roy, and Vermote 1998) and the global Web Enabled Landsat (WELD) product tiling system was used. The global WELD products define monthly and annual 30 m Landsat nadir BRDF-adjusted reflectance (NBAR) surface reflectance derived by the algorithms described in Roy et al. (2010, 2016) and are available at <http://globalweld.cr.usgs.gov/collections/>. The global WELD tiles are nested within the standard $10^\circ \times 10^\circ$ MODIS land product tiles (Wolfe, Roy, and Vermote 1998). There are 7×7 global WELD tiles within each MODIS land tile, and the file name includes the MODIS horizontal (0–36) and vertical (0–17) tile coordinates, and the nested WELD tile horizontal and vertical tile coordinates (0–6). Each global WELD tile is composed of 5295×5295 30 m pixels and covers about 159×159 km.

3.2. Reprojection and quantification of Sentinel-2 L1C geometric resampling shifts

The L1C 10 m data in the SAFE file were reprojected into the global WELD tile encompassing the majority of the SAFE file image area. Specifically, following the conventional inverse gridding approach (Konecny 1976), each 10 m pixel location (sinusoidal coordinates) across the global WELD tile was projected into the Sentinel-2 L1C tiles (UTM coordinates) taking care to use the correct L1C tile UTM zone. The reprojected locations usually fall between Sentinel-2 pixel locations and so nearest neighbour resampling was used as it is computationally efficient, preserves the input image pixel values and so raster cloud and saturation masks can be resampled, and because it allows for quantification of geometric resampling shifts. When considering a single image the maximum nearest neighbour resampling shift is 0.5 of the input image pixel dimension in the image x or y directions and $\sqrt{2}/2$ pixels in the input image diagonal directions (Shlien 1979; Roy 2000).

The correct handling of overlapping Sentinel-2 L1C tiles, and in particular of overlapping tiles that are defined in different UTM zones, is required to properly utilize and benefit from the Sentinel-2 L1C format. Figure 2 illustrates a cartoon of this issue for a projected sinusoidal tile pixel location (cross) and Sentinel-2 pixel locations for two adjacent spatially overlapping L1C tiles sensed in the same sensor swath but defined in different UTM zones (blue and red dots). The pixels in the two L1C tiles are illustrated with different colours and are not aligned because they are defined in different UTM zones. Under nearest neighbour resampling, the closest pixel to the cross is selected. In practice, the projected sinusoidal tile pixel locations could fall anywhere in the overlap region and the closest pixel could be from either Sentinel-2 L1C tile. In the illustrated example, the closest pixel is the red pixel that is distance a from the cross. If only the blue L1C tile pixels are considered, then the closest pixel is the blue pixel that is distance

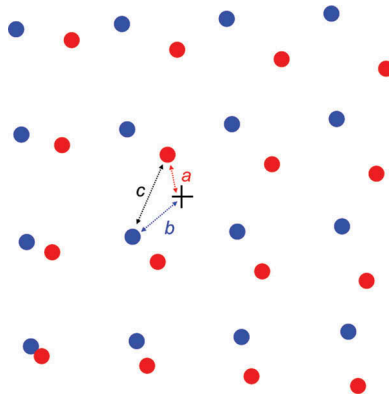


Figure 2. Cartoon of Sentinel-2 pixel locations on the earth surface for two adjacent overlapping L1C tiles sensed in the same MSI swath but defined in different UTM zones (blue and red dots) and the location of a projected sinusoidal tile pixel (cross). The distances a and b define nearest neighbour resampling errors, and c quantifies the position difference induced by considering one rather than the other tile of Sentinel-2 data (see text for details).

b from the cross. In Figure 2, the distances a and b correspond to location shift errors imposed by nearest neighbour resampling. The distance c quantifies the position difference induced by considering one rather than the other tile of Sentinel-2 data.

In this study, every 10 m global WELD tile pixel was reprojected into the SAFE file data and the distances a , b and c (Figure 2) were quantified where there were overlapping Sentinel-2 L1C tiles. The UTM zone East and North components of a and b were also derived. The distance c is more complex to determine as the tiles are defined in different UTM zones. Therefore, c was derived in metres using a spherical coordinate transformation as follows:

$$c = r \times \arccos(\sin\Phi_a \times \sin\Phi_b \times \cos(\lambda_a - \lambda_b) + \cos\Phi_a \times \cos\Phi_b) \times \pi/180 \quad (1)$$

where r is the semi-major Earth axis value used in the WGS84 UTM system (6378137.0 m), and λ_a , Φ_a and λ_b , Φ_b are the longitude and latitudes (decimal degrees), respectively, of the two earth surface pixel locations at either end of the arrow c in Figure 2.

3.3. Recommended projection and resampling methodology to correctly handle overlapping Sentinel-2 L1C tiles defined in different UTM zones

The recommended approach is to resample the data considering all the overlapping Sentinel-2 L1C tile pixels. In practice, this means either developing an efficient processing scheme, or storing all the Sentinel-2 L1C tile data in memory at the same time, which is computationally expensive given the very large SAFE file data volume and is complicated because of the need to handle the different UTM zones. A straightforward and recommended scheme is to process each Sentinel-2 L1C tile independently in sequence. For each resampled pixel location (i.e., the cross in Figure 2), the distance to the closest Sentinel-2 pixel is stored. Each time a resampled pixel location is projected into a Sentinel-2 tile, its distance to the closest Sentinel-2 pixel is derived and the Sentinel-2 pixel data are selected only if the distance is smaller than the distance found for the previous L1C tile. In this way, only one Sentinel-2 L1C tile at a time needs to be stored in memory, each UTM

zone is treated separately and the resampling results are the same regardless of the number or processing order of the overlapping Sentinel-2 L1C tiles. Thus, in the [Figure 2](#) example, if the first tile processed was the blue tile then the blue pixel data would be reprojected, and distance value b stored; then when the red tile is processed the resampled pixel location would be found to fall within the red tile and, as $a < b$, the red pixel data would be overwritten into the reprojected image.

4. Results

4.1. Example global WELD reprojected Sentinel-2 L1C data and quantification of the incidence of overlapping Sentinel-2 L1C tiles within SAFE files

[Figure 3](#) shows the reprojected Sudan Sentinel-2 data. Within the geographic extent of the global WELD tile, there were nine Sentinel-2 L1C tiles that were defined in two different UTM zones. Resampling effects are not apparent at this scale.

[Figure 4](#) shows the Sentinel-2 L1C tile counts for the Sudan SAFE tile data falling within the geographic extent of the WELD tile ([Figure 3](#)). There were a total of six Sentinel-2 tiles defined in UTM zone 35 N ([Figure 4\(a\)](#)) and three defined in UTM zone 36 N ([Figure 4\(b\)](#)). The overlapping Sentinel-2 tile boundaries occurring in each UTM zone are quite evident with up to four (yellow) different overlapping L1C tiles occurring at certain 10 m locations. A total of 19.04% ([Figure 4\(a\)](#)) and 12.37% ([Figure 4\(b\)](#)) of the 10 m pixel locations occurred where there were more than one overlapping Sentinel-2 tile defined in the same UTM zone, and 40.51% of the pixel locations occurred where

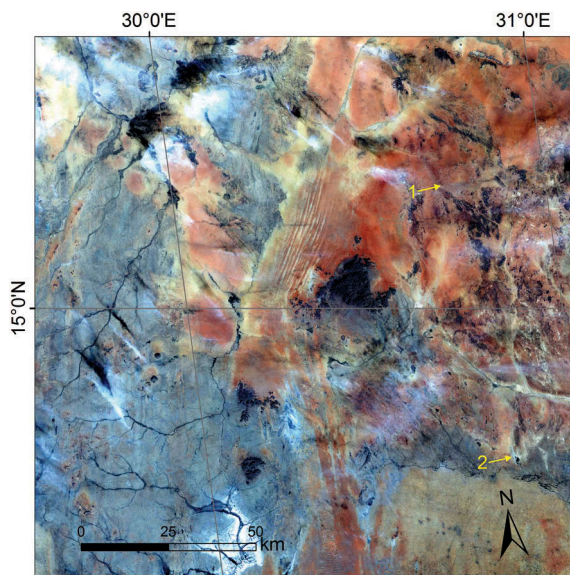


Figure 3. Sudan Sentinel-2 L1C SAFE file tile data (nine L1C tiles) reprojected into global WELD tile hh20vv07.h6v3 (sinusoidal projection, 15885×15885 10 m pixels) using the recommended method to handle overlapping Sentinel-2 L1C tile data defined in different UTM zones. True colour, i.e., 665 nm (red), 560 nm (green), 490 nm (blue), 10 m Sentinel-2 top of atmosphere reflectance bands shown. The numbered yellow arrows show the geographic locations of the results illustrated in [Figure 5](#).

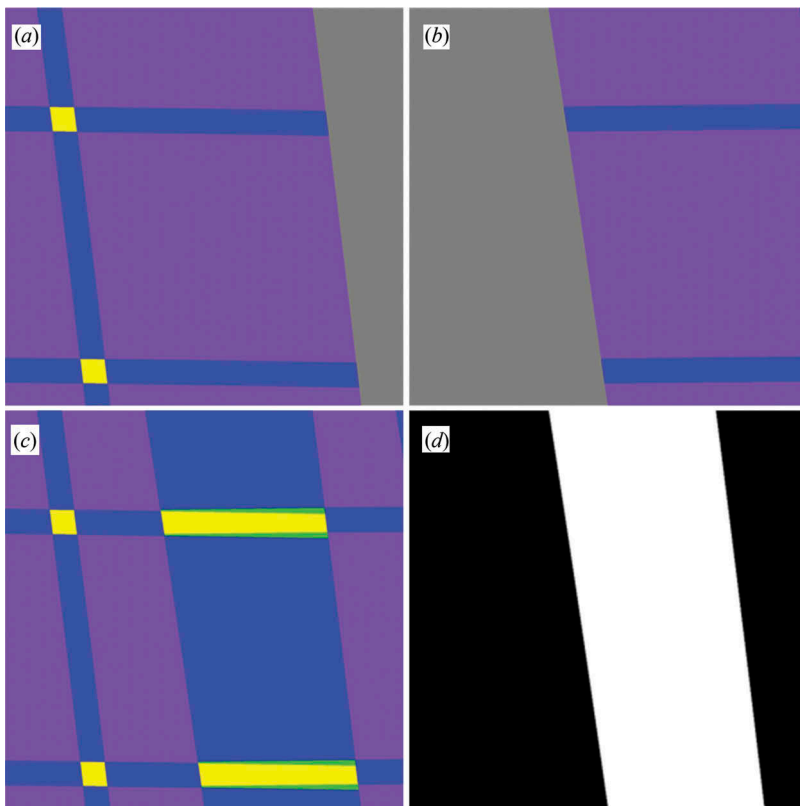


Figure 4. Sudan Sentinel-2 L1C tile counts for the same geographic region as [Figure 3](#). The counts of the number of different Sentinel-2 L1C tiles defined in UTM zone 35 N (a), in UTM zone 36 N (b), and in either zone (c), are coloured as Grey = 0, Purple = 1, Blue = 2, Green = 3, and Yellow = 4. Plot (d) shows the 10 m locations (white) where there were Sentinel-2 L1C tiles defined in both UTM zones.

overlapping Sentinel-2 tiles were defined in different UTM zones ([Figure 4\(d\)](#)). For the Russian Federation and South Africa tiles, between 5.79% and 14.43% of the pixel locations occurred where there were more than one overlapping Sentinel-2 tile defined in the same UTM zone, and between 47.53% and 48.98% of the pixel locations occurred where overlapping Sentinel-2 tiles were defined in different UTM zones.

4.2. Quantification of Sentinel-2 L1C geometric resampling shifts and detailed illustration of recommended resampling and reprojection approach

[Figure 4](#) illustrates the need for careful handling of the different L1C tiles found in each SAFE file. The finding that between 41% and 49% of the pixel locations in the global WELD tiles occurred where there were overlapping Sentinel-2 L1C tiles defined in different UTM zones underscores this need. The nearest neighbour resampling location shift errors, i.e., *a*, *b* and *c* ([Figure 2](#)), in the overlapping L1C tile regions were derived and are summarized in [Tables 1–3](#). The results are reported to the nearest millimetre, which is a false level of precision, but are reported to establish that the reprojection and resampling was implemented correctly and reflects the precision of the projection

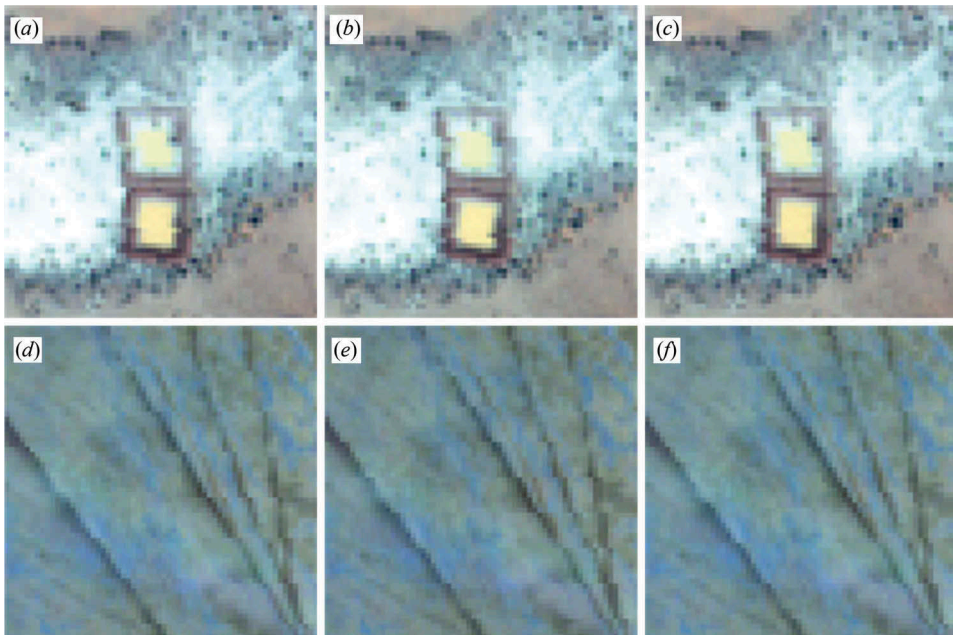


Figure 5. Example reprojected nearest neighbour resampled Sentinel-2 images considering (a and d) only one L1C tile defined in UTM zone 35 N (b and e) only one L1C tile defined in UTM zone 36 N (c and f), both overlapping tiles using the recommended resampling method. The images are all 250×250 10 m pixels and were derived from the Sudan SAFE file L1C data. Top row images (a–c) located at $15^{\circ}17'42.1''\text{N } 30^{\circ}39'48.9''\text{E}$ (Figure 3, location 1). Bottom row images (d–f) located at $14^{\circ}37'49.9''\text{N } 30^{\circ}43'40.5''\text{E}$ (Figure 3, location 2). True colour 665 nm (red), 560 nm (green) and 490 nm (blue) top of atmosphere reflectance shown.

calculations. For all three data sets, the UTM zone East and North components of a and b varied from about 0.0 m (i.e., the projected sinusoidal pixel coordinate fell precisely on a Sentinel-2 L1C pixel) to 5.0 m (i.e., the projected sinusoidal pixel coordinate fell midway between two Sentinel-2 L1C 10 m pixels). Similarly, the minimum and maximum values of a or b are bounded from approximately 0.0 m to $\sqrt{2}/2$ of the Sentinel-2 10 m pixel dimension. The mean and standard deviations of a and b are 3.836 m and 1.424 m. These statistics reflect the expected geometric resampling error when a single Sentinel-2 L1C 10 m tile is nearest neighbour resampled.

The distance c quantifies the shift induced by considering one UTM zone tile rather than the other UTM zone tile in regions where adjacent tiles overlap (Figure 2). For all three Sentinel-2 SAFE files, the minimum and maximum c values are about 0 m and not less than 13.9 m respectively, with mean and standard deviation values of about 5.2 m and 2.5 m, respectively, (Tables 1–3). Notably, the c value summary statistics are greater than the equivalent a and b statistics. This means that resampling and reprojection approaches that consider only the Sentinel-2 data from one L1C tile, and not from other tiles in the overlap region defined in different UTM zones, will result in a significant degradation of the geometric fidelity of the resampled image. This is illustrated in Figure 5 – the linear high contrast features are more coherent and the geometric fidelity is improved when the

Table 1. Summary statistics of Sentinel-2 L1C 10 m pixel nearest neighbour resampling shifts a , b , c (Figure 2) and the east and north components of a and b , for the Sudan SAFE file encompassed by global WELD tile hh20vv07.h6v3 (Figures 3 and 4).

	a_{east} (m)	a_{north} (m)	a (m)	b_{east} (m)	b_{north} (m)	b (m)	c (m) (" in parentheses)
Minimum	0.000	0.000	0.001	0.000	0.000	0.001	0.002 (0.0001")
Maximum	5.000	5.000	7.070	5.000	5.000	7.070	13.936 (0.4507")
Mean	2.500	2.500	3.826	2.500	2.500	3.826	5.225 (0.1690")
Standard deviation	1.443	1.443	1.424	1.443	1.443	1.424	2.484 (0.0803")

Statistics derived from a total of 252333225 10 m pixels where there were Sentinel-2 10 m data defined in both UTM zones 35 N and 36 N.

Table 2. Summary statistics of Sentinel-2 L1C 10 m pixel nearest neighbor resampling shifts a , b , c (Figure 2) and the east and north components of a and b , for the Russian Federation SAFE file encompassed by global WELD tile hh20vv03.h3v4.

	a_{east} (m)	a_{north} (m)	a (m)	b_{east} (m)	b_{north} (m)	b (m)	c (m) (" in parentheses)
Minimum	0.000	0.000	0.001	0.000	0.000	0.002	0.001 (0.0000")
Maximum	5.000	5.000	7.069	5.000	5.000	7.069	13.943 (0.4509")
Mean	2.500	2.500	3.826	2.500	2.500	3.826	5.208 (0.1684")
Standard deviation	1.443	1.443	1.424	1.443	1.443	1.424	2.476 (0.0801")

Statistics derived from a total of 223534923 10 m pixels where there were Sentinel-2 10 m data defined in both UTM zones 37N and 38N.

Table 3. Summary statistics of Sentinel-2 L1C 10 m pixel nearest neighbour resampling shifts a , b , c (Figure 2) and the east and north components of a and b , for the South Africa SAFE file encompassed by global WELD tile hh19vv12.h2v3.

	a_{east} (m)	a_{north} (m)	a (m)	b_{east} (m)	b_{north} (m)	b (m)	c (m) (" in parentheses)
Minimum	0.000	0.000	0.002	0.000	0.000	0.001	0.002 (0.0001")
Maximum	5.000	5.000	7.070	5.000	5.000	7.069	13.909 (0.4498")
Mean	2.500	2.500	3.826	2.500	2.500	3.826	5.217 (0.1687")
Standard deviation	1.443	1.443	1.424	1.443	1.443	1.424	2.480 (0.0802")

Statistics derived from a total of 166990903 10 m pixels where there were Sentinel-2 10 m data defined in both UTM zones 33S and 34S.

recommended method is used. The geometric differences among these three sets of images are greatest comparing the results derived from the separate L1C zone tiles, i.e., comparing the (a) and (b) results, or the (d) and (e) results. The recommended approach considers both sets of L1C data and therefore a greater density of Sentinel-2 observations is available for resampling (Figure 2), which results in the improved geometric fidelity evident in Figure 5(c,f).

5. Conclusion

The complexity of the Sentinel-2 L1C data format illustrated in this article presents some technical challenges and also opportunities. A significant proportion of the L1C tiles in each Sentinel-2 SAFE file (i.e., sensed in the same MSI swath) overlap and are defined in different UTM zones. Resampling and reprojection approaches that consider only the data from one L1C tile, and not from different UTM zone tiles in the tile overlap region, will fail to benefit from the increased information provided by the Sentinel-2 L1C format. Arguably, for certain applications, this may not matter, particularly those that derive coarser spatial resolution products than the native Sentinel-2 data resolution.

Reprojection approaches that consider only the Sentinel-2 data from one L1C tile, and not also from overlapping tiles defined in different UTM zones, will result in a pronounced degradation of the geometric fidelity of the reprojected data. Location shifts induced by considering one UTM zone L1C tile rather than the other UTM zone tile in regions where tiles overlap are shown to be greater than a single tile nearest neighbour resampling shifts. In solution, a recommended reprojection approach that considers all the L1C tile data, and therefore ensures that a greater spatial density of Sentinel-2 observations is available for resampling, was described. The recommended approach is computationally efficient, as it requires processing of each Sentinel-2 L1C tile independently, and properly utilizes and benefits from the L1C tile format. Other resampling approaches including bilinear and cubic convolution resampling that fit surfaces to the 4 and 16 neighbouring pixel values, respectively, in the input image to estimate the resampled pixel value (Park and Schowengerdt 1983) could be used to resample the projected Sentinel-2 L1C data. Regardless of which resampler is used, they are all expected to provide results with improved geometric fidelity if the greater density of Sentinel-2 observations in the L1C tile overlap region is resampled. Similarly, image restoration approaches that use knowledge of the system Point Spread Function (Shen et al. 2014) and pansharpener approaches that fuse higher spatial resolution panchromatic with lower spatial resolution multispectral imagery (Zhang and Roy 2016) may benefit.

Disclosure statement

No potential conflict of interest was reported by the authors.

Funding

This research was funded by the NASA Land Cover/Land Use Change (LCLUC14-2): Multi-Source Land Imaging Science Program, Grant NNX15AK94G, and by the U.S. Department of Interior, U.S. Geological Survey (USGS), Grant G12PC00069.

ORCID

David P. Roy  <http://orcid.org/0000-0002-1347-0250>

Jian Li  <http://orcid.org/0000-0003-0739-085X>

Hankui K. Zhang  <http://orcid.org/0000-0003-4470-3616>

Lin Yan  <http://orcid.org/0000-0002-8628-4395>

References

- Drusch, M., U. Del Bello, S. Carlier, O. Colin, V. Fernandez, F. Gascon, B. Hoersch, et al. 2012. "Sentinel-2: ESA's Optical High-Resolution Mission for GMES Operational Services." *Remote Sensing of Environment* 120: 25–36. doi:10.1016/j.rse.2011.11.026.
- ESA (European Space Agency). 2015a. "Sentinel-2 User Handbook, Issue 1, Rev 2, Revision 2." ESA Standard Document. Accessed July 24 2015, 64 pages.
- ESA (European Space Agency). 2015b. "Sentinel-2 Products Specification Document, Issue 13.1." ESA REF: S2-PDGS-TAS-DI-PSD. Accessed November 18 2015, 496 pages.
- Griffiths, P., S. Van Der Linden, T. Kuemmerle, and P. Hostert. 2013. "A Pixel-Based Landsat Compositing Algorithm for Large Area Land Cover Mapping." *IEEE Journal of Selected Topics in Applied Earth Observations and Remote Sensing* 6: 2088–2101. doi:10.1109/JSTARS.2012.2228167.
- Konecny, G. 1976. "Mathematical Models and Procedures for the Geometric Registration of Remote Sensing Imagery." *International Archives of Photogrammetry and Remote Sensing* 21: 1–33.
- Park, S. K., and R. A. Schowengerdt. 1983. "Image Reconstruction by Parametric Cubic Convolution." *Computer Vision, Graphics, and Image Processing* 23 (3): 258–272. doi:10.1016/0734-189X(83)90026-9.
- Roy, D. P. 2000. "The Impact of Misregistration upon Composited Wide Field of View Satellite Data and Implications for Change Detection." *IEEE Transactions on Geoscience and Remote Sensing* 38: 2017–2032. doi:10.1109/36.851783.
- Roy, D. P., J. Ju, K. Kline, P. L. Scaramuzza, V. Kovalsky, M. Hansen, T. R. Loveland, E. Vermote, and C. Zhang. 2010. "Web-Enabled Landsat Data (WELD): Landsat ETM+ Composited Mosaics of the Conterminous United States." *Remote Sensing of Environment* 114: 35–49. doi:10.1016/j.rse.2009.08.011.
- Roy, D. P., M. A. Wulder, T. R. Loveland, C. E. Woodcock, R. G. Allen, M. C. Anderson, D. Helder, et al. 2014. "Landsat-8: Science and Product Vision for Terrestrial Global Change Research." *Remote Sensing of Environment* 145: 154–172. doi:10.1016/j.rse.2014.02.001.
- Roy, D. P., H. K. Zhang, J. Ju, J. L. Gomez-Dans, P. E. Lewis, C. B. Schaaf, Q. Sun, J. Li, H. Huang, and V. Kovalsky. 2016. "A General Method to Normalize Landsat Reflectance Data to Nadir BRDF Adjusted Reflectance." *Remote Sensing of Environment* 176: 255–271. doi:10.1016/j.rse.2016.01.023.
- Shen, H., W. Zhao, Q. Yuan, and L. Zhang. 2014. "Blind Restoration of Remote Sensing Images by a Combination of Automatic Knife-Edge Detection and Alternating Minimization." *Remote Sensing* 6: 7491–7521. doi:10.3390/rs6087491.
- Shlien, S. 1979. "Geometric Correction, Registration and Resampling of Landsat Imagery." *Canadian Journal of Remote Sensing* 5: 74–89. doi:10.1080/07038992.1979.10854986.
- Snyder, J. P. 1993. *Flattening the Earth: Two Thousand Years of Map Projections*. Chicago: The University of Chicago Press.
- Wolfe, R., M. Nishihama, A. Fleig, J. Kuyper, D. Roy, J. Storey, and F. Patt. 2002. "Achieving Sub-Pixel Geolocation Accuracy in Support of MODIS Land Science." *Remote Sensing of Environment* 83: 31–49. doi:10.1016/S0034-4257(02)00085-8.
- Wolfe, R., D. P. Roy, and E. Vermote. 1998. "MODIS Land Data Storage, Gridding, and Compositing Methodology: Level 2 Grid." *IEEE Transactions on Geoscience and Remote Sensing* 36: 1324–1338. doi:10.1109/36.701082.
- Yan, L., D. P. Roy, H. K. Zhang, J. Li, and H. Huang. 2016. "An Automated Approach for Sub-Pixel Registration of Landsat-8 Operational Land Imager (OLI) and Sentinel-2 Multi Spectral Instrument (MSI) Imagery." *Remote Sensing* 8: 520. doi:10.3390/rs8060520.
- Zhang, H. K., and D. P. Roy. 2016. "Computationally Inexpensive Landsat 8 Operational Land Imager (OLI) Pansharpening." *Remote Sensing* 8: 180. doi:10.3390/rs8030180.